Preparation and Characterization of Waterborne Polyurethane/Clay Nanocomposite: Effect on Water Vapor Permeability

Mohammad Mizanur Rahman,[1] Han-Do Kim,[2] Won-Ki Lee[1]

[1]*Division of Chemical Engineering, Pukyong National University, Busan 608-739, Korea*
[2]*Department of Organic Material Science and Engineering, Pusan National University, Busan 609-735, Korea*

Received 1 August 2007; accepted 4 July 2008
DOI 10.1002/app.28985
Published online 17 September 2008 in Wiley InterScience (www.interscience.wiley.com).

ABSTRACT: A series of waterborne polyurethane (WBPU)/clay nanocomposite coating materials were prepared by prepolymer process with different clay contents (0–2 wt %). The study investigated surface structure as well as water resistance, thermal, mechanical, and water vapor permeability (WVP) of composite materials as a function of clay contents. The glass transition temperature of composite materials was higher than pristine WBPU and also increased with increasing clay contents. Thermal stability, and water resistance of the nanocomposite films also increased, when compared with pristine WBPU, and these properties increased with an increase in clay content. The maximum tensile strength was found with optimum clay content (1 wt %) of composite films. The WVP of coated nylon fabrics depend on the clay content and temperatures. The rate (%) of WVP of coated nylon fabrics decreased with increasing clay content at a fixed temperature. However, at a fixed clay content the WVP increased with the increase of temperatures. © 2008 Wiley Periodicals, Inc. J Appl Polym Sci 110: 3697–3705, 2008

Key words: polyurethanes; clay; nanocomposites

INTRODUCTION

The polymer/clay nanocomposites have attracted much more attention in recent decades because of their unique properties compared with those of the conventional composites.[1] Among those properties are higher strength and modulus,[1,2] better dimensional and thermal stability,[3,4] as well as improved barrier property and chemical stability.[4,5] The polymer/clay nanocomposites can be generally classified into two groups. The intercalated polymer/clay nanocomposites have layered clay dispersed in a polymer matrix with polymer chains inserted into clay layers that retain their lateral order. The exfoliated ones consist of fully delaminated clay platelets dispersed individually in the matrix. Thus, each platelet interacts with the matrix and improves the properties of the nanocomposites more effectively.

Waterborne polyurethane (WBPU) is considered as an important alternative material to solvent-based polyurethane for various applications such as coating for wood finishing, glass fiber sizing, automotive topcoats and adhesives due to increasing awareness of health and environmental safety.[6–11] However, the WBPU is deficient in chemical resistance, thermal resistance, and tensile strength compared with its counterpart solvent-based polyurethane. Many different methods have been employed to overcome these disadvantages of WBPU such as hydrophobic monomers grafted to polyurethane (PU) main chain,[12,13] the change of the type and content of ionic centers,[14–16] the adjustment of the ionic neutralization degree,[17–19] the blending,[20–22] and copolymerization of different polymers,[23–27] and crosslinking.[28,29]

The water vapor permeability (WVP) of WBPU coating materials is one of the major challenging issues on many different sectors such as textile, medicine, and biotechnology.[30–34] With respect to practical applications, the coating materials required high thermal stability, hydrolytic stability, and better mechanical property (tensile strength and initial modulus). Unfortunately, few coating materials satisfied the above requirements and also are very scarce due to unfavorable combinations of price, processibility, and performance. This type of coating materials are often made and used for specialized applications, and are not commonly available commercially.

Recently, the thermal and mechanical properties are improved by making polyurethane clay

Correspondence to: H.-D. Kim (kimhd@pusan.ac.kr) or W.-K. Lee (wonki@pknu.ac.kr).

Contract grant sponsor: Pukyong National University.
Contract grant sponsor: Korea Science and Engineering Foundation (KOSEF) [funded by the Korea government (MOST)]; contract grant number: R01-2006-000-10042-0.

nanocomposite materials.[35–37] However, a few reports are found on WBPU/clay nanocomposite in open literature.[38–41] In this study, we prepared WBPU/clay nanocomposite coating materials by prepolymer process at various clay contents (0–2 wt %) using organoclay Cloisite 15A. We characterized the surface structure of nanocomposite films by SEM and TEM. The affect of clay content on glass transition temperature and storage modulus was evaluated. We investigated the particle size of dispersion, as well as water resistance, thermal stability, and mechanical properties of WBPU/clay nanocomposite films. We also evaluated the WVP of coated nylon fabrics at different temperature (20–80°C) using the prepared WBPU/clay nanocomposite coating materials.

EXPERIMENTAL

Materials

Poly(tetramethylene oxide glycol) (PTMG, number–average molecular weight $M_n = 2000$ g/mol; Aldrich Chemical) was vacuum dried at 90°C and 1–2 mmHg for 3 h before use. 2,2-Dimethylolpropionic acid (DMPA, Aldrich Chemical, Milwaukee, WI), triethylamine (TEA; Junsei Chemical, Tokyo, Japan), *N*-methyl-2-pyrrolidone (NMP; Junsei Chemical), 4,4-dicyclohexylmethane diisocyanate (H_{12}MDI, Aldrich Chemical), and ethylene diamine (EDA, Junsei Chemical) were used after dehydration with 4-Å molecular sieves for one week. Dibutyltin dilaurate (DBTDL, Aldrich Chemical), thickener (L75N, Bayer, Leverkusen, Germany), and hardener (ARF 30, polyisocyanate 20 wt %, Dongsung NSC, Korea) were used without further purification. The clay, Cloisite®15A containing 125 mequiv/100 g clay of quaternary ammonium ions, was kindly donated by Southern Clay Products (Gonzales, TX).

Preparation of WBPU/clay nanocomposite dispersions

The WBPU/clay nanocomposite dispersions were prepared by prepolymer mixing process (Scheme 1). During preparation, at first PTMG was placed in a four-necked flask equipped with a thermometer, a stirrer, a condenser with a drying tube, an inlet for dry nitrogen, and a heat jacket and was degassed in vacuum at 80°C for 30 min. Clay was mixed with polyol and stirred at 85°C for 3 h. DMPA/NMP (1/1 w/w) was added to the flask, and the mixture was allowed to cool to 40°C under moderate stirring (175–200 rpm). Then, DBTDL (1 drop) and H_{12}MDI were added to the flask, and the reaction continued for 3 h at 85°C. The change of NCO value during reaction was determined with the standard dibutylamine back-titration method (ASTM D 1638). Then, methyl ethyl ketone (MEK, 20 wt %) was added to decrease the viscosity of the reaction mixture. TEA was added to the reaction mixture to neutralize the carboxyl group of the NCO-terminated polyurethane prepolymer. After 30 min of neutralization, distilled water (70 wt %) was added to the reaction mixture with vigorous stirring (1300–1500 rpm). The dispersion was chain-extended by dropping of EDA/H2O (1/13 w/w) at 40°C for 1 h, and the reaction continued until the NCO peak (2270 cm^{-1}) in the IR spectra had completely disappeared. All of the WBPU/clay nanocomposite dispersions (30 wt % solid content) were obtained after evaporation of MEK.

Preparation of WBPU/clay nanocomposite films

The WBPU/clay nanocomposite films were prepared by pouring the aqueous dispersion on a Teflon disk and dried under the ambient conditions for 48 h. The films (typically about 0.5-mm thick) were dried in vacuum at 60°C for 1 day and stored in a desiccator at room temperature.

Preparation of WBPU/clay nanocomposite-coated nylon fabrics

The coating materials were formulated from nanocomposite dispersions, thickner (0.5 wt %) and hardener (0.5 wt %). The coating materials were coated onto the nylon fabrics using steel bar and then dried at 100°C for 5 min. The thickness of the coated layer was about 0.08 mm.

Characterization

The X-ray diffraction (XRD) patterns were recorded using a Philips Xpert XRD System at a voltage of 40 kV, and a radiation of wavelength 1.542 Å. Diffraction patterns were obtained in the range of Bragg's angle $2\theta = 0°–40°$. The 2θ scan rate was 2°/min.

The scanning electron microscopy (SEM) micrographs of WBPU/clay nanocomposite films were obtained with a Hitachi (Japan) *S*-4200 field emission scanning electron microscope at 5 kV.

A Hitachi model H-7500 transmission electron microscope was used to examine the morphology of the samples. The samples for transmission electron microscopy (TEM) examination were first prepared by the placement of the nanocomposite films in epoxy capsules and the curing of the epoxy at 70°C for 24 h in an oven. The cured epoxies containing WPU/clay nanocomposites were then microtomed with a diamond knife into 70–90 nm thick slices at −100°C. Finally, a 3-nm thick carbon layer was deposited on these slices on 200-mesh copper nets for TEM observation.

The mean particle size of WBPU/clay nanocomposite dispersions were measured using laser-scattering equipment (Autosizer, Melvern IIC, Malvern,

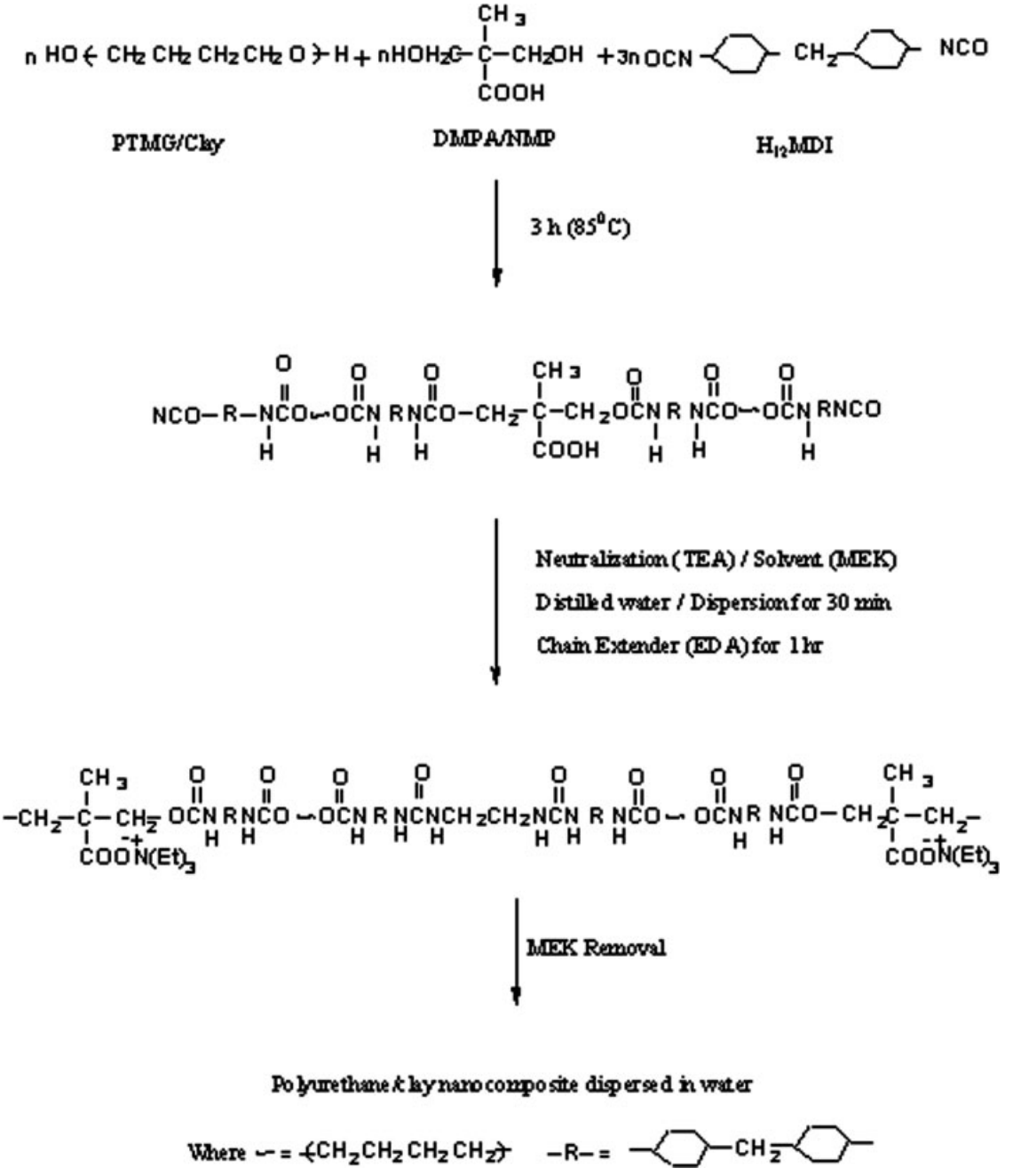

Scheme 1 The preparation process for WBPU/clay nanocomposite dispersion.

Worcester, UK). The average particle diameters were measured at 25°C.

Water swelling of the WBPU/clay nanocomposite films was evaluated to measure the water resistivity of the film. The films were immersed in water for 24 h at 25°C. Three parallel measurements were carried out for each sample. The water swelling of the films was calculated by

$$\text{Swelling } (\%) = \frac{W - W_0}{W_0} \times 100$$

where W_0 is the weight of the dried film, and W is the weight of the film at equilibrium swelling.

The thermal behavior of the WBPU/clay nanocomposite film was analyzed by differential scanning calorimetry (DSC; model 220C, Seiko, Chibas, Japan). 3–4 mg of the film was placed in an aluminum pan and the experiment was carried out under nitrogen gas atmosphere at a heating rate of 10°C/min from −70 to 300°C and then quenched to −70°C at an average cooling rate of 20°C/min using liquid nitrogen. The second thermal scan was taken over a temperature range of −70 to 300°C with a heating

TABLE I
Sample Designation and Composition of WBPU/Clay Nanocomposite Dispersions

Sample designation	Composition (molar ratio)					Clay (Cloisite 15A) (wt %)
	PTMG	DMPA	H_{12}MDI	TEA	EDA	
WBPU 0	2.00	1.10	4.10	1.10	1.00	0.0
WBPU 1	2.00	1.10	4.10	1.10	1.00	0.50
WBPU 2	2.00	1.10	4.10	1.10	1.00	1.00
WBPU 3	2.00	1.10	4.10	1.10	1.00	2.00

rate of 10°C/min.

The thermal dynamic mechanical behavior of the WBPU/clay nanocomposite film was measured at 4 Hz with a dynamic mechanical thermal analyzer (DMTA MK III, Rheometrics Scientific, Surrey, UK) with a heating rate of 3°C/min. The dimension of the film sample was $5 \times 5 \times 0.2$ mm^3 for dynamic mechanical thermal analysis measurement. The mechanical measurements were made in simple extension on dumbbell specimens with a tensile tester (Tinius Olsen 1000, PA) at a crosshead speed of 20 mm/min according to ASTM D 412.

Thermal gravimetry analysis (TGA) was performed in a Pyris 6 TGA (Perkim Elmer, USA). 5.0 mg of WBPU film was placed in a platinum pan and heated from 30 to 500°C under N_2, at a heating rate of 10°C/min.

The tensile test was measured at room temperature with a United Data System tension meter (SSTM-1 United Data Systems, Instrom, Japan) according to the ASTM D 638 specifications. A crosshead speed of 30 mm/min was used throughout these investigations to determine the ultimate tensile strength and initial modulus and the elongation at break for all the samples. The values quoted are the average of five measurements.

The WVP was examined by using an evaporation method described in ASTM E 9663-T.

RESULTS AND DISCUSSION

The sample designation and composition of WBPU/clay nanocomposite is shown in Table I. The WBPU/clay nanocomposites were prepared with various clay contents (0–2 wt %). The XRD analysis (Fig. 1) of WBPU/clay nanocomposite was conducted to identify the surface structure (exfoliated or intercalated). Each WBPU/clay nanocomposite exhibits a broad, amorphous diffraction halo at $2\theta = 19.26°$, and similar to pristine WBPU. This diffraction halo is associated with amorphous phase of WBPU. The characteristic peak of the clay Cloisite 15A is disappeared in WBPU/clay nanocomposite. This indicates that most of the clay platelets might be exfoliated.[38] For many solvent-based PU nanocomposites with the absence of ions in PU moieties, the electrostatic forces between the clay platelets have a tendency to squeeze the PU polymer chains out and subsequently result is an intercalated structure. The clay intercalated with the PU polymer exhibits a reflection at $2\theta = 2.5°$, for a certain solvent-based polyurethane nanocomposite.[36,37] In the WBPU/clay nanocomposite system studied in this work, the above squeeze effect has been overcome by the ionic attractions between anionic WBPU and cationic clay platelets.[38,39] Therefore, the intercalated WBPU polymer chains can peel the platelets away from the well-intercalated silicate stacks or tactoids, and this result might be an exfoliated silicate system.

Although XRD is by far the simplest method available to measure the dispersion state of clay in WBPU/clay nanocomposite, SEM is also used to visually evaluate the clay dispersion and the amount of aggregation of clay platelets. The efficiency of the clay in modifying the properties of the matrix polymer is primarily determined by the degree of its dispersion in the polymer matrix. The aggregated clay morphology can be characterized with SEM. Because of the difference in scattering density between the clay and polyurethane, large clay aggregates can be easily imaged in SEM. SEM of the WBPU/clay nanocomposite films are compared in Figure 2. WBPU 0 shows the pristine WBPU surface, whereas in WBPU 2 and WBPU 3 the homogeneously dispersed clay particles in the matrix are observed. However, the

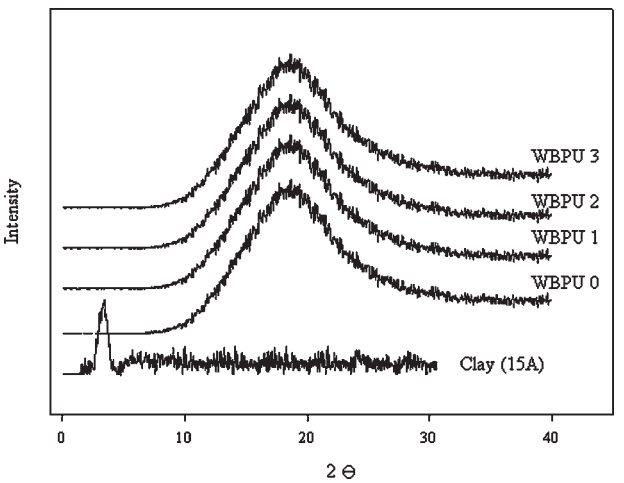

Figure 1 XRD of WBPU/clay nanocomposite films.

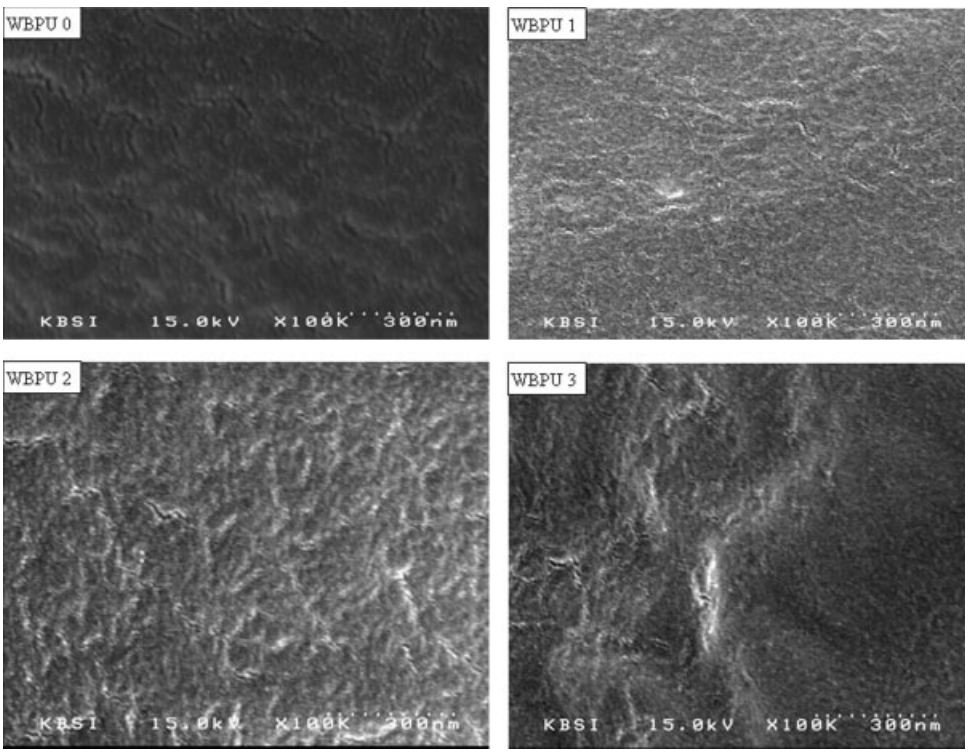

Figure 2 SEM photographs of WBPU/clay nanocomposite films.

surface of WBPU 3 with higher clay content (2 wt %) showed some deformed portions that may result from the aggregation of some clay particles in the WBPU/clay nanocomposite film.

The actual surface structure of a nanocomposite can be observed using TEM images. Figure 3 shows typical images of WBPU/clay nanocomposites with various clay contents. As shown in these images the structure of the nanocomposite depends on clay

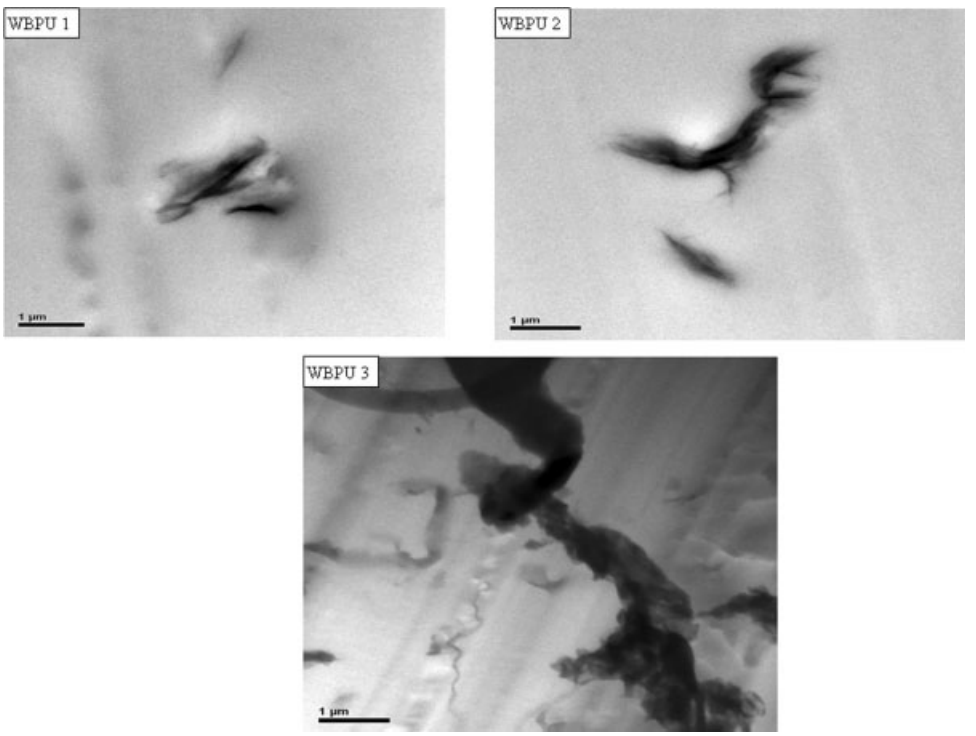

Figure 3 TEM photographs of WBPU/clay nanocomposite films.

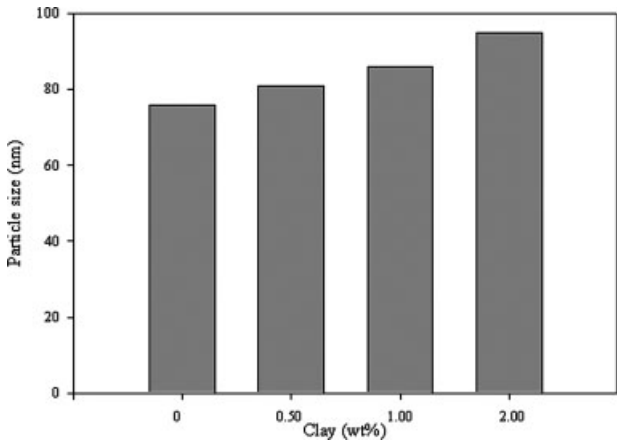

Figure 4 Effect of clay content on the particle size of WBPU/clay nanocomposite dispersions.

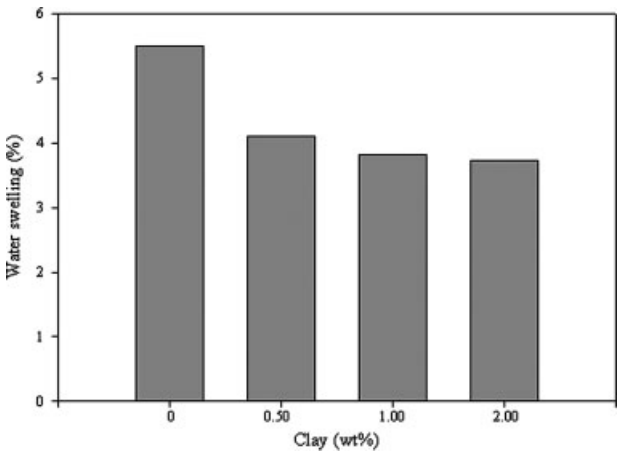

Figure 5 Water swelling (%) of WBPU/clay nanocomposite films.

contents. The mixtures of intercalated and exfoliated structures were found with 0.50 wt % and 1.0 wt % clay in WBPU 1 and WBPU 2, respectively. However, the structure with 2 wt % clay (WBPU 3) is different than 0.50 wt % (WBPU 1) and 1.0 wt % (WBPU 2) clay loaded nanocomposites. Some clusters or agglomerated clay particles are observed due to higher clay loaded WBPU/clay nanocomposite. It was shown before that the typical peak of Cloisite 15A in XRD of WBPU/clay nanocomposites disappeared. This disappearance could be explained either by the exfoliation of the silicate or by a high disorder of the clay.[42] If the silicate layers were exfoliated, the *d*-spacing would become too high and could not be detected by the XRD methods. Moreover, if the clays were not well ordered, it would fail to produce a Bragg diffraction peak.[43]

The mean particle size of WBPU/clay nanocomposite dispersion is shown in Figure 4. It was found that the mean particle size of dispersion was increased with increasing clay content. The increase of the mean particle size was due to two factors, such as, hydrophobic nature of the clay component[39,40,44] and the decrease of electrostatic force of carboxyl acid salt group.[38] Relatively larger particles are preferred in surface coating due to rapid drying and the prepared WBPU/clay nanocomposite material could be used as a coating material due to larger mean particle size.[34]

The water resistance of WBPU/clay nanocomposite films was determined by water swelling test. The corresponding results are shown in Figure 5. It was found that the water swelling (%) decreased with increasing clay contents. It implies that the hydrophilicity of the film was decreased with increasing clay contents. This is because of hydrophobic surface of clay in WBPU/clay nanocomposites.[40,41] Moreover, the organoclay layers being dispersed in nanometer scale in polyurethane matrix and resist to water molecule pass through the polyurethane composite. When the addition of organoclay was 1 wt %, the water swelling of composite film was decreased from 5.80% to 3.70%.

The thermal property of WBPU/clay nanocomposite film was studied by differential scanning calorimeter (DSC) (Fig. 6). The enthalpy and melting temperature of soft segments are summarized in Table II. It was found that all the samples showed an endothermic melting peak for soft segment (PTMG). The melting temperature was almost same position at 18°C. This indicates that the phase mixing of soft segment with hard segment was almost not occurred and remains same condition with various clay contents. The melting temperature of hard segment was not observed indicating the amorphous structure of hard segment region of WBPU/clay nanocomposite. May be the presence of clay disrupts

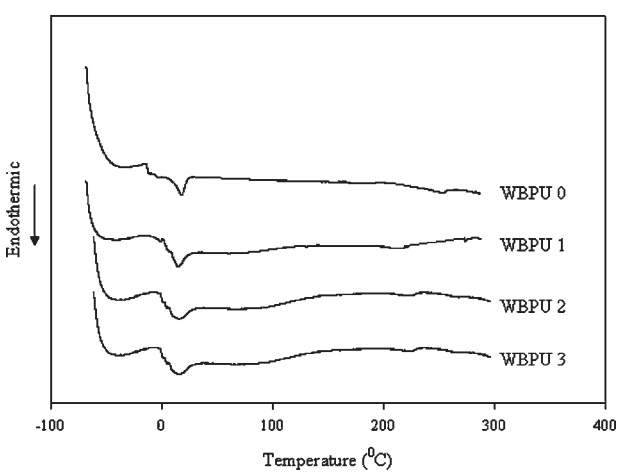

Figure 6 DSC of WBPU/clay nanocomposite films.

TABLE II
Thermal Properties of WBPU/Clay Nanocomposite Films

Sample Designation	T_m SS (°C)	ΔH_m SS (mJ/mg)	Temperature (°C) at various residue (wt %)		
			10%	20%	40%
WBPU 0	18.9	18.0	318.24	349.42	388.12
WBPU 1	18.1	21.6	320.05	351.00	390.70
WBPU 2	18.0	26.0	332.29	359.20	393.52
WBPU 3	18.0	26.5	335.22	365.97	397.72

the hard segment crystallinity, and the peak for hard segment was not found. Moreover lower hard segment content (20 wt %) as well as randomly oriented DMPA make the amorphous structure of hard segment. The heat of fusion for soft segment (ΔH_m SS) was found to be increased with increasing clay contents. This indicates that a little crystallinity in soft segment (PTMG) still remains in all of the samples; moreover the crystallinity increased with increasing clay contents. May be the dispersed silicate layers in WBPU/clay nanocomposite served as nucleation seeds that induced some additional crystallinity in PTMG soft segment.[45] During the second heating DSC run (not shown), the melting peak for soft segment was not found indicating that the crystallization kinetic was very slow of the WBPU/clay nanocomposites. The slow crystallization of the WBPU/clay nanocomposite might be due to the dispersed clay layers.

Figure 7 presents the storage modulus (E') and tan δ of the nanocomposite films. The storage modulus, E', and tan δ of WBPU/clay nanocomposites are compared with that of pristine WBPU. The nanocomposites have higher E' values than those of pristine WBPU over the whole temperature range and E' of nanocomposites increase with an increase of organoclay content of nanocomposites [Fig. 7(a)]. The improvement of the storage modulus with small clay loading may have resulted from the strong interaction between the organoclay and the polymer matrix. Figure 7(b) shows two damping (transition) peaks for WBPU/clay nanocomposites. The peaks are ascribed to the glass transition temperature of the soft and hard-segments of the nanocomposites. The dominant peak around at 112°C represent the glass transition of the hard-segment and the weak broad peak around at −52 to −44°C are the glass transition temperature of the soft-segment portion of the WBPU/clay nanocomposite. The T_g of WBPU/clay nanocomposite materials increases gradually along with the clay contents. This is tentatively attributed to the confinement of the intercalated polymer chains within the clay galleries, which prevents the segmental motions of the polymer chains.

TGA is a good method to determine the thermal stability of the WBPU/clay nanocomposite films. The TGA curves (Fig. 8) for all samples indicate that there are two stages of decomposition. The temperature for various weight loss (%) of WBPU/clay nanocomposite is summarized in Table II. The increase of the thermal stability could be attributed to the high thermal stability of the clay and the interaction between the clay particles and the PU-urea matrix.[46] Because the chain motions of polymer molecules in these silicate layers were barred and limited, therefore, thermal stability of the nanocomposites increased.[47] The other probable cause will be

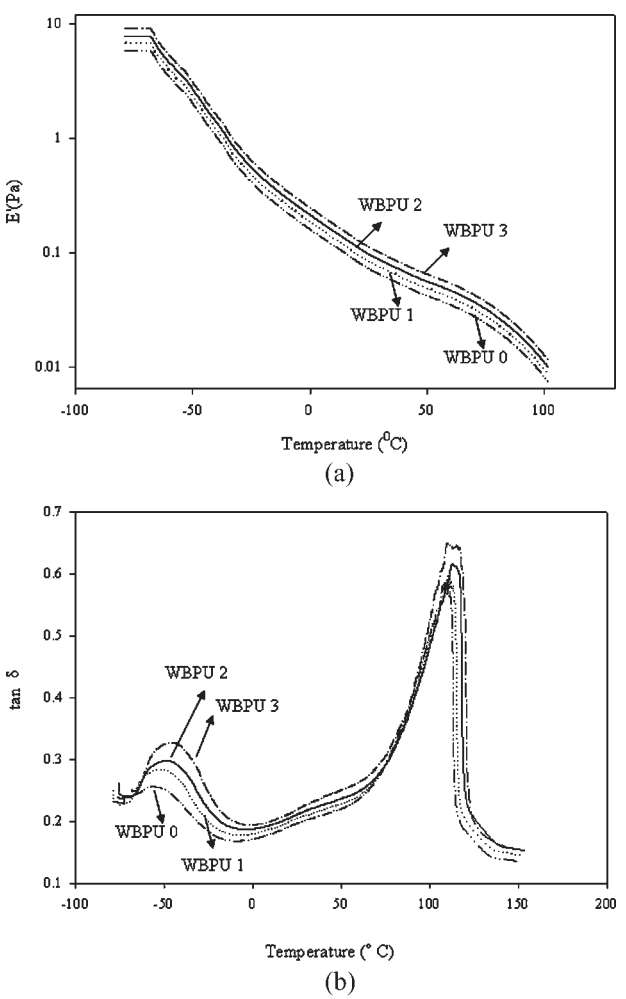

Figure 7 (a) Storage modulus of WBPU/clay nanocomposite films. (b) Tan δ of WBPU/clay nanocomposite films.

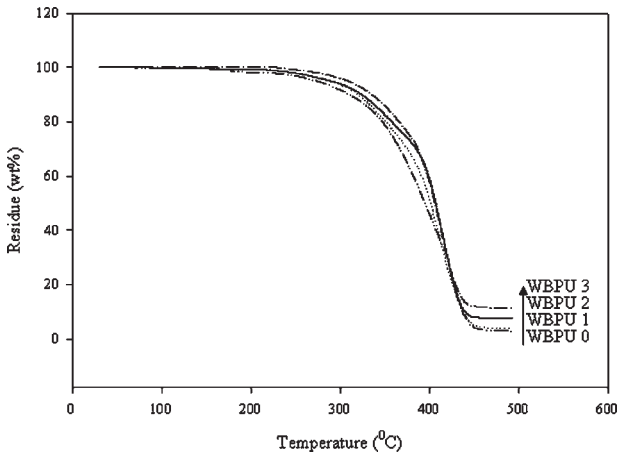

Figure 8 TGA thermographs of WBPU/clay nanocomposite films.

the layered silicates make the path longer for escaping of the thermally decomposed volatiles, or in other words clay particles can enhance the thermal stability of the polymer by acting as thermal insulator and mass transport barrier to the volatile products generated during decomposition.[48,49]

To investigate the effect of clay contents on mechanical properties (tensile strength and initial modulus) of WBPU/clay nanocomposite films, the tensile test was carried out (Fig. 9). The corresponding tensile properties are summarized in Table III. It was found that the clay content has a remarkable effect on mechanical properties. The tensile strength and initial modulus were increased up to the optimum clay content. It is evident that even the presence of a small amount of clay (0.5 wt %) would largely improve the tensile properties. The WBPU/clay nanocomposite containing 0.5 wt % and 1.0 wt % clay, the tensile strength increased about 4 and 7%, respectively, comparing to pristine WBPU. Similarly the initial modulus increased 17 and 200% for 0.5 wt %

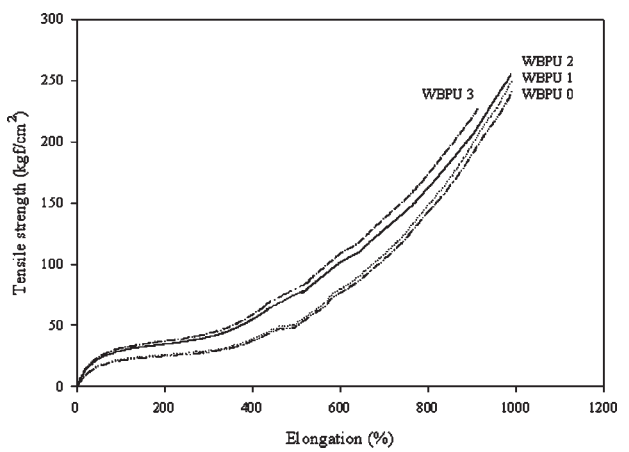

Figure 9 Mechanical properties (tensile strength) of WBPU/clay nanocomposite films.

TABLE III
Mechanical Properties of WBPU/Clay Nanocomposite Films

Sample designation	Tensile strength (kgf/cm^2)	Initial modulus (kgf/cm^2)	Elongation at break (%)
WBPU 0	240	6	991
WBPU 1	250	7	990
WBPU 2	256	18	989
WBPU 3	227	20	912

and 1 wt % clay in WBPU/clay nanocomposite, respectively. The higher tensile strength and initial modulus were due to interaction of the pristine polyurethane and the nanometer clay layers. However, the tensile strength decreased with 2 wt % clay content in WBPU/clay nanocomposite. This is probably due to some degree of aggregation of clay platelets (confirmed by SEM and TEM). Similar trends have been noted in other publications also.[41,50]

In Figure 10 the WVP of coated nylon fabrics is shown. The WVP of WBPU/clay nanocomposite coating materials are lower than those for the pristine WBPU coating material. It was found that the WVP of coated nylon fabrics decreased with increasing clay contents. The WVP of this series was decreased in the order: WBPU 0 > WBPU 1 > WBPU 2 > WBPU 3. This result is attributed to the plate-like clays that effectively increase the length of the diffusion pathways and decrease the WVP of coated nylon fabrics. The tight chain packing (confirmed by DMA) of the composite materials also favor to decrease the WVP of coated nylon fabrics. The rate of WVP (%) at various temperatures is summarized in Table IV. The WVP of coated nylon fabrics was increased with increasing temperature. The polymer chain is changed to loosely bind by increasing temperature leads to the significant

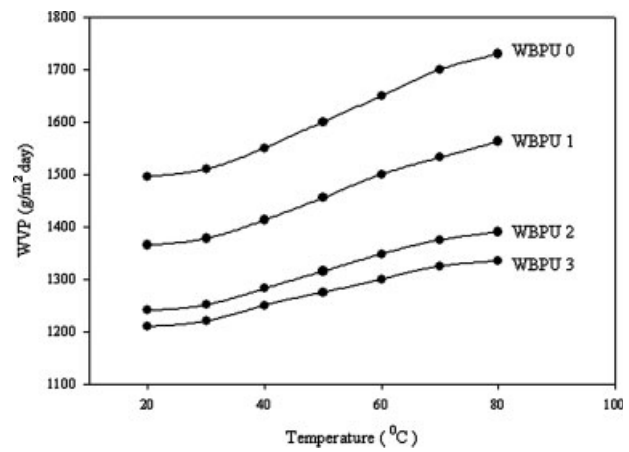

Figure 10 Water vapor permeability as a function of temperature of coated nylon fabrics using WBPU/clay nanocomposite coating material.

TABLE IV
Rate of WVP (%) of Coated Nylon Fabrics at Various Temperatures

	WVP (%) at different temperature (°C)					
Sample designation	30	40	50	60	70	80
WBPU 0	0.94	3.61	6.95	10.30	13.64	15.64
WBPU 1	0.92	3.51	6.59	9.89	12.23	14.50
WBPU 2	0.88	3.39	6.05	8.70	10.88	12.10
WBPU 3	0.83	3.30	5.37	7.44	9.50	10.33

increase in diffusion and permeation of small penetrants through the WBPU coating nylon fabrics.[33] However, the low increasing rate of WVP was found with higher clay content.

CONCLUSIONS

WBPU/clay nanocomposite coating materials were prepared with various clay contents. The surface structure of composite films depends on clay content. Low clay loaded WBPU/clay nanocomposite (WBPUA1/WBPUA2) film showed mixture of intercalated and exfoliated structure, whereas high clay loaded (WBPUA3) composite film showed agglomerated structure. The T_g of composite films were higher than pristine WBPU, moreover, the T_g increased with increasing clay contents. The thermal stability and water resistance of composite films also increased with increasing clay contents. The rate of WVP of coated nylon fabrics gradually decreased with increasing clay content of WBPU/clay nanocomposite material. However, the WVP rate was increased with the increase of temperature at a fixed clay content.

References

1. Messersmith, P.; Giannelis, E. P. Chem Mater 1994, 6, 1719.
2. Lan, T.; Pinnavaia, T. J Chem Mater 1994, 6, 2216.
3. Wang, Z.; Pinnavaia, T. J Chem Mater 1998, 10, 1820.
4. Massam, J.; Wang, Z.; Pinnavaia, T. Z.; Lan, T.; Beall, G. Polym Mater Sci Eng 1998, 78, 274.
5. Massam, J.; Pinnavaia, T. J Mater Res Soc Symp Proc 1998, 520, 223.
6. Chen, G. N.; Chen, K. N. J Appl Polym Sci 1997, 63, 1609.
7. Diterich, D.; Keberie, W.; Witt, H. Angew Chem Int Ed Engl 1970, 9, 40.
8. Coutinho, F. M. B.; Delpech, M. C. Polymer Testing 1996, 15, 103.
9. Delpech, M. C.; Coutinho, F. M. B. Polym Test 2000, 19, 939.
10. Shao, C. H.; Huang, J. J.; Chen, G. N.; Yeh, J. T.; Chen, K. N. Polym Degrad Stab 1999, 65, 359.
11. Coutinho, F. M. B.; Delpech, M. C. Polym Degrad Stab 2000, 70, 49.
12. Kim, D. K.; Lee, S. B.; Doh, K. S.; Nam, Y. W. J Appl Polym Sci 1999, 74, 2029.
13. Gooch, J. W.; Dong, H.; Schork, F. J. J Appl Polym Sci 2000, 76, 105.
14. Lim, C. H.; Choi, H. S.; Noh, S. T. J Appl Polym Sci 2002, 86, 3322.
15. Turri, S.; Levi, M.; Trombetta, T. J Appl Polym Sci 2004, 93, 136.
16. Kim, C. K.; Kim, B. K. J Appl Polym Sci 1991, 43, 2295.
17. Jang, J. Y.; Jhon, Y. K.; Cheong, I. W.; Kim, J. H. Colloids Surf A 2002, 196, 135.
18. Yang, J. E.; Kong, J. S.; Park, S. W.; Lee, D. J.; Kim, H. D. J Appl Polym Sci 2002, 86, 2375.
19. Kim, B. K.; Kim, T. K.; Jeong, H. M. J Appl Polym Sci 1994, 62, 371.
20. Hirose, M.; Zhou, J.; Nagai, K. Prog Org Coat 2000, 38, 27.
21. Bremner, T.; Hill, D. J. T.; Killen, M. I.; O'Donnell, J. H.; Pomery, P. J.; St. John, D.; Whittaker, A. K. J Appl Polym Sci 1997, 65, 939.
22. Yen, M. S.; Tsai, P. Y. J Appl Polym Sci 2003, 90, 233.
23. Kim, B. K.; Lee, J. C.; Lee, K. H. J Macromol Sci Pure Appl Chem 1994, 31, 1241.
24. Zhuang, H. Z.; Camberlin, A.; Hercules, D. M. Macromolecules 1997, 30, 1153.
25. Adhikari, R.; Gunatillake, P. A.; McCarthy, S. J.; Meijs, G. F. J Appl Polym Sci 1999, 74, 2979.
26. Kim, B. K.; Lee, J. C. J Polym Sci Part A: Polym Chem 1996, 34, 1095.
27. Ahn, T. O.; Jung, S. U.; Jeong, H. M.; Lee, S. W. J Appl Polym Sci 1994, 51, 43.
28. Kwon, J. Y.; Kim, H. D. Macromol Res 2006, 14, 373.
29. Mequanint, K.; Sanderson, R. Polymer 2003, 44, 2631.
30. Chen, G. H.; Hoffman, A. S. Nature 1995, 373, 49.
31. Stern, S. A. J Membr Sci 1994, 94, 1.
32. Lomax, G. R. Tex Asia 2001, 39.
33. Kwak, Y. S.; Park, S. W.; Lee, Y. H.; Kim, H. D. J Appl Polym Sci 2003, 89, 123.
34. Yun, J. K.; Yoo, H. J.; Kim, H. D. J Appl Polym Sci 2007, 105, 1168.
35. Gorrasi, G.; Tortora, M.; Vittoria, V. J Polym Sci Part B: Polym Phys 2005, 43, 2454.
36. Chang, J. H.; An, Y. U. J Polym Sci Part B: Polym Phys 2002, 40, 670.
37. Xu, R.; Manias, E.; Snyder, A. J Macromolecules 2001, 34, 337.
38. Lee, H. T.; Hwang, J. J. J Polym Sci Part A: Polym Chem 2006, 44, 5801.
39. Lee, H. T.; Lin, L. H. Macromolecules 2006, 39, 6133.
40. Kim, B. K.; Seo, J. W.; Jeong, H. M. Eur Polym J 2003, 39, 85.
41. Rahman, M. M.; Yoo, H. J.; Mi, C. J; Kim, H. D. Macromolecular Symp 2007, 249–250, 251.
42. Ishida, H.; Campbell, S.; Blackwell. J Chem Mater 2001, 12, 1260.
43. Solarski, S.; Benali, S.; Rochery, M.; Devaux, E.; Alexandre, M.; Monteverde, F.; Dubois, P. J Appl Polym Sci 2005, 95, 238.
44. Rahman, M. M.; Kim, H. D. J Appl Polym Sci 2006, 102, 5684.
45. Chen, T. K.; Tien, Y. I.; Wei, K. H. J Polym Sci Part A: Polym Chem 1999, 37, 2225.
46. Kim, D. S.; Kim, J. T.; Woo, W. B. J Appl Polym Sci 2005, 96, 1641.
47. Ni, P.; Li, J.; Suo, J; Li, S. J Appl Polym Sci 2004, 94, 534.
48. Takeichi, T.; Guo, Y. J Appl Polym Sci 2003, 90, 4075.
49. Choi, W. J.; Kim, S. H.; Kim, Y. J.; Kim, S. C. Polymer 2004, 45, 6045.
50. Ma, J.; Zhang, S.; Qi, Z. J Appl Polym Sci 2001, 82, 1444.